Virology 450-451 (2014) 222–232

Contents lists available at ScienceDirect

Virology

journal homepage: www.elsevier.com/locate/yviro

Repair of the 3′ proximal and internal deletions of a satellite RNA associated with *Cucumber mosaic virus* is directed toward restoring structural integrity

Sun-Jung Kwon [1,2], Sonali Chaturvedi [1], A.L.N. Rao *

Department of Plant Pathology & Microbiology, University of California, Riverside, CA 92521-0122, United States

ARTICLE INFO

Article history:
Received 7 November 2013
Returned to author for revisions
29 November 2013
Accepted 8 December 2013
Available online 7 January 2014

Keywords:
3′ repair
Satellite RNA
RNA virus
Cucumovirus

ABSTRACT

The phenomenon of rapid turnover of 3′ proximal nucleotides (nt) lost by the action of nuclease in RNA viruses is integral to replication. Here, a set of six deletions encompassing the 3′ 23 nt region of a satellite RNA (satRNA) of *Cucumber mosaic virus* (CMV) strain Q (Q-sat), were engineered. Repair of the 3′ end was not observed in the absence of CMV. However, co-expression with CMV in planta revealed that Q-sat mutants lacking the 3′ 18 nt but not the 3′ 23 nt are repaired and the progeny accumulation was inversely proportional to the extent of the deletion. Progeny of the 3′Δ3 mutant were repaired to wild type (wt) while those from the remaining four mutants were heterogeneous, exhibiting a wt secondary structure. Analysis of additional 3′ internal deletions mutants revealed that progeny with a repaired sequence reminiscent of wt secondary structure were competent for replication and systemic spread.

Introduction

In RNA viruses, replication of genomic RNA is one of the fundamental steps in the infection cycle. Since the 3′ ends of viral genomic RNAs encompass sequences that are intimately involved in proper translation and recognition by RNA-dependent RNA polymerase (RdRp) to initiate minus-strand synthesis, their integrity must be maintained. To meet this requirement and to prevent the loss of the critical 3′ end nucleotides due to the action of cellular nucleases, viral RNAs have evolved to undergo a repair process by a variety of mechanisms that involve either viral RdRp, tRNA nucleotidyltransferase, RNA recombination or abortive initiation products (Hema et al., 2005; Nagy et al., 1997; Rao et al., 1989; Rao and Hall, 1993). Whatever the mechanism, the 3′ ends of viral genomes are functionally analogous to telomeres of chromosomal DNA (Burgyan and Garcia-Arenal, 1998; Hema et al., 2005; Rao et al., 1989; Weiner and Maizels, 1987).

Genomic RNAs of plant infecting RNA viruses terminate at their 3′ ends in a variety of structures such as stem-loop (e.g. *Alfalfa mosaic virus*) (Bol, 2005), poly A tracts (e.g. potyviruses) or tRNA-like structures (e.g. *Brome mosaic virus*, BMV) (Dreher, 2009). The mechanism regulating the 3′-end repair was extensively studied in BMV and *Turnip crinkle virus* (TCV). In BMV, the repair of the 3′-CCA_{OH} terminal trinucleotide sequence is mediated through either polymerase error, RNA recombination or by the action of cellular (ATP, CTP): tRNA nucleotidyltransferase (Hema et al., 2005; Rao et al., 1989; Rao and Hall, 1993). Whereas in TCV, abortive products generated by viral RdRp mediate the repair of the 3′ end (Nagy et al., 1997).

Cucumber mosaic virus (CMV) is a tripartite icosahedral virus and represents the type member of the *cucumovirus* genus (Palukaitis and Garcia-Arenal, 2003). Its genome is divided among three single-stranded positive sense RNAs (ssRNA), collectively encoding four non-structural proteins and one structural protein. CMV RNAs 1 and 2 encode replicase subunits 1a and 2a, respectively (Palukaitis and Garcia-Arenal, 2003). In addition, genomic RNA2 also encodes another gene product, 2b, the designated suppressor of RNA silencing (Ding et al., 1994). The two gene products encoded by dicistronic RNA3 are dispensable for viral replication but are required for infectivity in plants (Boccard and Baulcombe, 1993). A nonstructural protein of 30 kDa, encoded by the 5′ half of RNA3 is the designated movement protein (MP) required for cell-to-cell movement (Palukaitis and Garcia-Arenal, 2003). The 20-kDa CP, encoded by the 3′ half of CMV RNA3, is translated from subgenomic RNA4 transcribed from progeny minus-sense RNA3 (Boccard and Baulcombe, 1993).

In addition to the genomic and subgenomic RNAs, some strains of CMV contain another small, non-coding RNA referred to as a satellite. Inherently satellite RNA (satRNA) is unable to replicate by itself and is therefore completely dependent on the replication

* Corresponding author. Tel.: +1 951 827 3810.
E-mail address: arao@ucr.edu (A.L.N. Rao).
[1] These authors contributed equally to the work.
[2] Present address: Horticultural and Herbal Crop Environment Division, National Institute of Horticultural and Herbal Science, RDA, Suwon 441-440, Republic of Korea.

0042-6822/$ - see front matter © 2013 Elsevier Inc. All rights reserved.
http://dx.doi.org/10.1016/j.virol.2013.12.008

machinery of CMV, the helper virus. A hallmark feature of satRNAs is the lack of detectable nucleotide sequence homology with their helper virus (Hu et al., 2009). The 5′ capped satRNAs are 330 to 405 nucleotides long (Garcia-Arenal and Palukaitis, 1999; Simon et al., 2004) and often interfere with helper virus replication and modulate the course of disease development in plants incited by their helper virus(Hu et al., 2009; Shimura et al., 2011; Smith et al., 2011). Because of this biological significance, satRNAs have been used as model systems for understanding how macromolecules interact with their plant host and cause disease (Hu et al., 2009; Shimura et al., 2011; Smith et al., 2011; Wang et al., 2004). An earlier study performed in determining the mechanism involved in maintaining the integrity of the satRNA genome revealed that mutants lacking the 3′-most-7 but not 12 nucleotides, are repaired in a template independent manner exclusively by CMV, but not *Tomato aspermy virus* (TAV, another member of the genus cucumovirus) replicase (Burgyan and Garcia-Arenal, 1998).

Infectivity in mammalian cells with a cloned DNA from the RNA genome was shown for poliovirus (Racaniello and Baltimore, 1981). Later, mechanical inoculation of CaMV 35S promoter driven cDNA copies of RNA genome components of CMV (Ding et al.,1995), BMV (Mori et al., 1991) and *Tomato mosaic virus* (Weber et al., 1992) also resulted in efficient infections that are indistinguishable from infections with in vitro transcripts. In all these cases, RNA synthesis is initiated in the nucleus. In the context of plant viruses, one of the major drawbacks of the mechanical inoculation, specifically for a multicomponent virus such as CMV, is that only a limited number of cells receive the required constellation of viral components to initiate viral replication. Thus, *Agrobacterium*-mediated transient expression (agroinfiltration) is a powerful approach that combines the advantages of T-DNA-based RNA transcription and synchronized delivery of multiple plasmids to the same cell. Using this agroinfiltration, we and others have consistently showed that replication (Annamalai and Rao, 2005; Annamalai et al., 2008; Gopinath and Kao, 2007; Kwon and Rao, 2012; Yi et al., 2009) and cytopathological phenotypes exhibited by BMV genome components delivered by agroinfiltration (Bamunusinghe et al., 2013, 2011) are identical to those resulting from mechanical inoculations. Furthermore, agroinfiltration has been successfully used for studying RNA recombination (Marillonnet et al., 2004) and RNAsilencing studies (Li et al., 2002). Thus, results obtained by agroinfiltration are not artifacts. It should be considered as a technical advancement in achieving the synchronized delivery of multiple plasmids to a majority of plant cells. Therefore, the rationale of this study is to evaluate whether the 3′ end repair could be extended beyond the 3′-most-7 nucleotides if the helper virus replicase and each 3′ terminal deletion mutant sequences are co-expressed in a majority of the cells delivered via agroinfiltration which is unlikely to happen with mechanical inoculation. Consequently, in this work, we compared the relative 3′ end repair of satRNA by its helper virus replicase in plants receiving the inoculum by agroinfiltration. Furthermore, unlike a previous study (Burgyan and Garcia-Arenal, 1998), progeny recovered from inoculated and un-inoculated systemically infected *Nicotiana benthamiana* leaves were sequenced. Collectively the results show that a requirement to restore the 3′ structural integrity allows helper virus replicase to extend the repair of 3′ proximal deletions of satRNA up to 18 nt as well as internal deletions.

Results

Characteristics of 3′ proximal deletion mutants of Q-satRNA

All mutants constructed in this study (Fig. 1) are engineered into the genetic background of a T-DNA based wild type (wt) agroconstruct of Q-satRNA (Qs-wt; Fig. 1). To determine the minimal repairable 3′-proximal nucleotides of Q-satRNA in planta

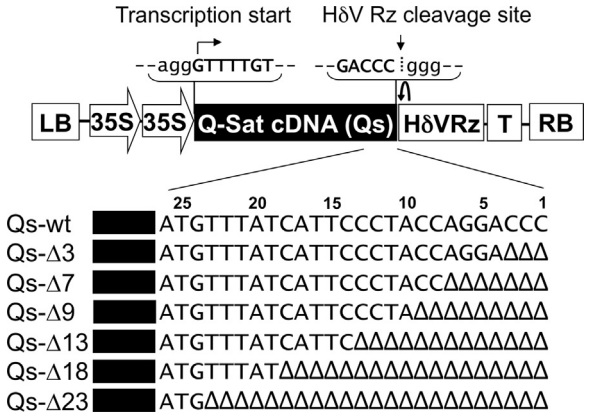

Fig. 1. Characteristic features of T-DNA based constructs of Q-sat variants used in this study and their stability in vivo. Schematic representation of aT-DNA based wt Q-sat (Qs) agrotransformant is shown. The position of the double 35S promoters (arrows) at the 5′end and positions of the hepatitis delta virus (HδV) ribozyme (Rz) and the 35S terminator (T) at the 3′ end are shown. At the 5′ junction, the nucleotide sequence of the 35S promoter (lowercase letters) and the 5′sequence of Q-sat (uppercase letters) are shown. A bent arrow indicates the expected transcription start site. At the 3′end, viral sequence (uppercase letters) left after self-cleavage by the HδV Rz are shown. An arrow shows the predicted self-cleavage site. The 3′ 26 nt sequence in Qs-wt and each variant is shown. The deleted nt in 3′Δ3, 3′Δ7, 3′Δ9, 3′Δ13, 3′Δ18 and 3′Δ23 variants are indicated by Δ.

by its helper virus, a set of six deletion mutants characterized by lacking the 3′ terminal 3 nucleotides (nt) (Qs-Δ3), 7 nt (Qs-Δ7), 9 nt (Qs-Δ9), 13 nt (Qs-Δ13), 18 nt (Qs-Δ18) or 23 nt (Qs-Δ23) was assembled. Cloning of wt and each deletion mutant cDNAs was designed such that the *de novo* synthesized RNA transcripts would terminate with the expected 3′ terminus and will not have any non-viral nucleotides due to the presence of a self-cleaving ribozyme sequence of *Hepatitis delta virus* (HDV) (Fig. 1).

Ectopically expressed Q-sat 3′ deletions are not repaired by cellular polymerase

It has been conclusively demonstrated that ectopic expression via agroinfiltration would result in the accumulation of viral and satRNAs to detectable levels in the absence of sustained replication (Annamalai and Rao, 2005; Choi et al., 2012; Gopinath and Kao, 2007; Seo et al., 2013). In principle, 35S driven T-DNA based transient expression is initiated in the nucleus by cellular polymerase. Therefore prior to testing helper virus-mediated repair of satRNA, it is imperative to verify whether transiently expressed satRNA mutants are repaired by the cellular polymerase before exiting into the cytoplasm. To test this possibility, we performed the following experiments. In the first experiment, plants were infiltrated with agrotransformants of wt and each 3′ terminal deletion mutant of Q-satRNA without helper virus and total RNA was isolated at 4 dpi and subjected to Northern blot hybridization. Results shown in Fig. 2A revealed that the stability of a given mutation reflected by its detection in Northern blots is inversely proportional to the extent of the engineered deletion. Among six deletion mutants, ectopically expressed RNA transcripts corresponding to three mutants (Qs-Δ3, Qs-Δ7, and Qs-Δ9) were accumulated to detectable levels, although the relative levels, compared to wt, varied between 78% and 19% (Fig. 2A). Prolonged exposure of the Northern blot failed to detect RNA bands corresponding to mutants Qs-Δ13, Qs-Δ18, and Qs-Δ23 (data not shown).

To verify the preservation of the engineered deletions, we performed two RT-PCR assays. In the first assay total RNA isolated from *N. benthamiana* leaves infiltrated with above-mentioned mutant inocula was subjected to poly-A tailing followed by RT-PCR and sequenced as described under Materials and methods section. Results shown in Fig. 2B revealed that compared to the wt control, RT-PCR

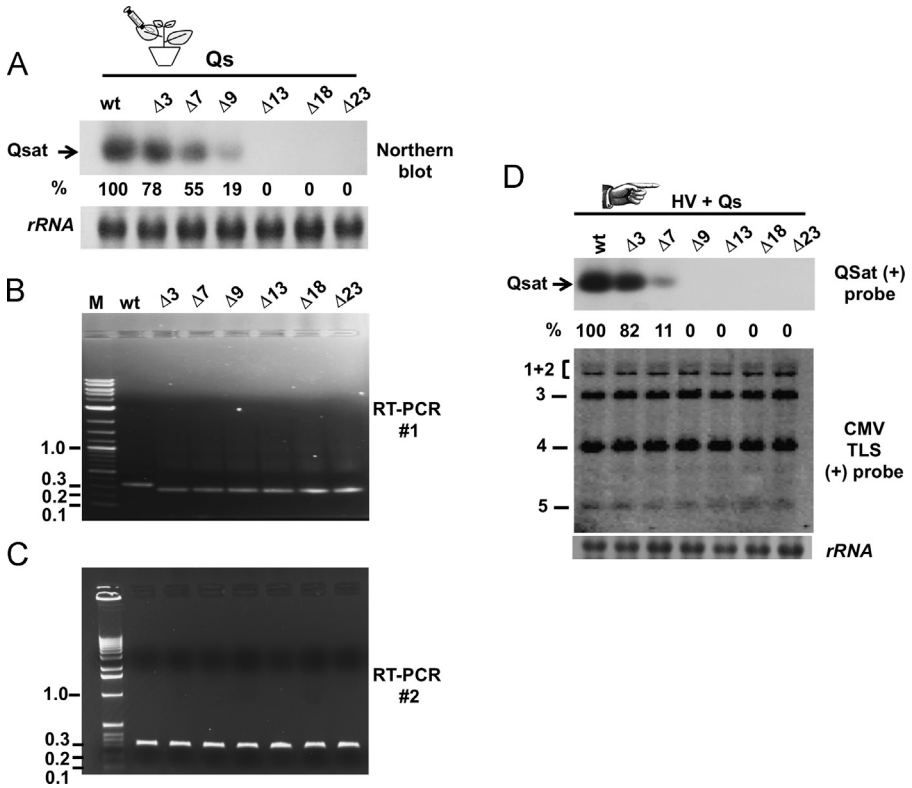

Fig. 2. Stability of Q-sat variants. (A) Agrotransformants of Qsat wt and each 3′ deletion variant was autonomously agroinfiltrated in *Nicotiana benthamiana* leaves and total RNA extracted at 4 dpi was subjected to Northern blot hybridization with a ^{32}P-labelled riboprobe designed to detected Qsat (+). Phosphoimaging was used to quantitate the accumulation levels of each 3′ deletion variant transcript. Loading controls are represented by ribosomal RNA (rRNA). (B) Agarose gel electrophoretic analysis of products of RT-PCR #1 assay. Total RNA isolated from agroinfiltrated leaves was treated with RNase-free DNAse to digest T-DNA templates and the resulting products were electrophoresed on PAGE-Urea gels, RNA bands of desired size were excised, eluted, poly A tailed and subjected to RT-PCR using a set of 3′ primer complementary to poly A tail and a forward primer complementary to 5′ Qsat RNA as described under Materials and methods section. A 5 μl sample of each RT-PCR product was subjected to agarose gel electrophoresis. (C) Agarose gel electrophoretic analysis of products of RT-PCR #2 assay. Following PAGE-Urea analysis of total RNA as described above, excised RNA bands were subjected to RT-PCR using 3′ primers specific for each deletion mutant and a forward primer complementary to 5′ Qsat RNA. (D) Replication of Qsat variants in mechanically inoculated plants. Total RNA recovered from leaves autonomously expressing indicated Qsat mutants were mixed with helper virus (HV) RNA and mechanically inoculated to *N. benthamiana*. At 5 dpi, duplicate blots containing the total. RNA isolated from inoculated leaves were subjected to Northern blot hybridization with ^{32}P-labelled riboprobes specific for either Qsat or CMV RNAs using 3′ conserved region (CMV TLS) as shown on the right of each panel. The positions of Qsat RNA or RNA1 to RNA5 of helper virus are indicated on the left of each panel. rRNA represent a loading control. Accumulation levels of Qsat RNA below the upper panel were normalized against wt Qsat as 100%.

product of each 3′ terminal deletion mutant migrated faster than the 300 nt size marker (Fig. 2B). Sequencing results showed that in each case the 3′ end deletion was extended between 116 to 148 nt (Qs-Δ3, 116 nt deleted; Qs-Δ7, 115 nt deleted; Qs-Δ9, 112 nt deleted; Qs-Δ13, 145 nt deleted; Qs-Δ18, 137 nt deleted and Qs-Δ23, 148 nt deleted). These results suggested that, in the absence of helper virus, ectopically expressed 3′ deletion mutants are unstable and were subjected to extended 3′truncations by cellular RNase. However, a possibility exists that the original engineered mutant population could exist at a low percentage that is hard to recover by the above used procedure. To verify this we used a second RT-PCR assay that was performed with a set of 5′ and 3′ primers that was used to engineer each deletion (see Materials and methods section). Migration profiles of RT-PCR products shown in Fig. 2C suggest that ectopically expressed RNA transcripts of each mutant were present in infiltrated *N. benthamiana* leaves. Direct sequencing of these RT-PCR products confirmed the preservation of each engineered deletion. Taken together the results suggested cellular polymerase did not modify the engineered deletions during transient expression originated in the nucleus.

Repair of 3′ end mutants of Q-satRNA by helper virus in mechanically inoculated leaves

Total RNA recovered from infiltrated *N. benthamiana* leaves autonomously expressing Qs-Δ3, Qs-Δ7, Qs-Δ9, Qs-Δ13, Qs-Δ18, and Qs-Δ23 (Fig. 2A) were mixed with helper virus and mechanically inoculated to *N. benthamiana* and total RNA recovered at 4 dpi was subjected to Northern blot hybridization. Replication profiles of each Q-sat 3′ terminal deletion mutant in mechanically inoculated plants shown in Fig. 2D are identical to those reported by Burgyan and Garcia-Arenal (1998). For example, among six deletion mutants tested, only the progeny of Qs-Δ3 was accumulated to near wt level (82%) while that of Qs-Δ7 remained low (11%) (Fig. 2D). No progeny RNA was detected for the remaining four mutants, even when the blots were exposed for a prolonged period. Progeny sequence of Qs-Δ3, and Qs-Δ7 recovered from these mechanically inoculated plants revealed that for Qs-Δ3,100% of Q-sat progeny (10/10 clones sequenced) had regained the deleted wt 3′ CCC sequence. Whereas, for Qs-Δ7, among 10 clones, unlike wt (^{7}AGGACCC^{1}), 50% displayed the presence of a uracil at position 7 and absence of the 3′ C residue (^{7}UGGACCΔ^{1}) while the remaining 50% displayed ^{7}UGGAΔΔΔ^{1} sequence. Lack of near perfect 3′ terminal sequences explain why the progeny of Qs-Δ7 accumulated poorly. However, total and virion RNA of Qs-Δ3 and Qs-Δ7 recovered at 10 dpi from systemically infected *N. benthamiana* leaves had perfect wt sequence (data not shown). Collectively, the results shown in Fig. 2(A–D) suggested that sequence restoration seen for 3′ deletion mutants is exclusively mediated by helper virus replicase, as suggested previously (Burgyan and Garcia-Arenal, 1998).

Agroinfiltration extends the 3′ end repair of Q-satRNA by helper virus to 18 nt

Unlike mechanical inoculation, agroinfiltration offers the advantage of synchronized delivery of multiple components of the inoculum to the same cell (Annamalai and Rao, 2005). Furthermore, agroinfiltration results in transient expression of T-DNA genes up to 7 days (Kapila et al., 1997), a feature critical for analyzing the biological activity of mutants that are less-stable (Fig. 2A). Therefore, to verify whether repair of the 3′ deletions in Q-satRNA could be extended if mutant transcripts are continuously available as substrates for the helper virus replicase in the same cell, liquid agrocultures of each Q-sat 3′ terminal deletion mutant was mixed with agrocultures of three helper virus genome components and infiltrated into *N. benthamiana* leaves. At 4 dpi total RNAs were extracted from these infiltrated leaves and subjected to Northern blot analysis.

In contrast to previous results obtained from mechanical inoculation (Fig. 2D) (Burgyan and Garcia-Arenal, 1998), an interesting RNA profile was observed when Q-sat mutant progeny recovered from agroinfiltrated *N. benthamiana* leaves were analyzed by Northern blot hybridization (Fig. 3A and B). Detectable level of progeny RNA, indicative of 3′ end repair, was evident for five of the six mutants. Compared to a high-level accumulation of the control infiltration performed with the Qs-wt (100%; Fig. 3A, lane 3), the accumulation of monomeric (1 ×) and dimeric (2 ×) forms of Q-satRNA progenies decreased gradually as the length of the 3′ terminal deletions increased from 3 to 18 (69% to 3%; Fig. 3A lanes 4–8). No progeny accumulation was detected for the mutant lacking the 3′ terminal 23 nt (Qs-Δ23; Fig. 3A lane 9). This replication profile for each deletion mutant was consistently observed in three additional repeated experiments.

In addition to infiltrated leaves of *N. benthamiana*, the upper systemically infected leaves were also analyzed two weeks after agroinfiltration. For example, by contrast to infiltrated leaves (Fig. 2A), in systemically infected leaves, similar levels of monomeric and dimeric forms of Q-satRNA progenies were accumulated for Qs-wt and Qs-Δ3 (100% vs 91%; Fig. 3B, lane 3 and 4). The relative accumulation levels of Qs-Δ7, Qs-Δ9 and Qs-Δ13 did not significantly differ from mutants in infiltrated leaves (compare Fig. 3A and B). Although Qs-Δ18 accumulated to almost similar levels to that of Qs-Δ13 (3% vs 4%) in infiltrated leaves, it failed to accumulate in systemically infected leaves (compare lanes 8 in Fig. 3A and B). Since mutant Qs-Δ23 did not accumulate in infiltrated leaves, it was not detected in systemically infected leaves either (compare lanes 9 in Fig. 3A and B).

To verify the extent of repair that occurred in each case, mutant progeny corresponding to monomeric size in infiltrated (at 4 dpi) and systemically infected (at 15 dpi) *N. benthamiana* leaves was gel-purified, cloned and sequenced. Results are summarized in Table 1. Qs-Δ3 progeny recovered from both local as well as systemically infected leaves terminated with CCC_{OH} (Table 1) indicating that the 3 deleted 3′ nucleotides had been completely restored to wt sequence. It is likely that the 3′ end repair could have occurred during the early phases of replication since 100% of the clones analyzed had wt sequence (Table 1). By contrast, sequencing of the progeny recovered from infiltrated and systemically infected leaves for mutants Qs-Δ7, Qs-Δ9 and Qs-Δ13 revealed that, despite a majority of the sequences that terminated in CCC_{OH}, the 3′ end repair had generated imperfect progeny exhibiting heterogeneity within the 3′ 13 nt region (Table 1). For example, in 50% (5 of 10 clones) of the Qs-Δ7 progeny recovered from infiltrated *N. benthamiana* leaves, the deleted sequence was repaired with $^{7}GGGUCCC^{1}_{OH}$. This sequence is different from that of wt ($^{7}AGGACCC^{1}_{OH}$) by having a guanine residue for adenine at position 7 and a uracil for adenine at position 4. Whereas 80%

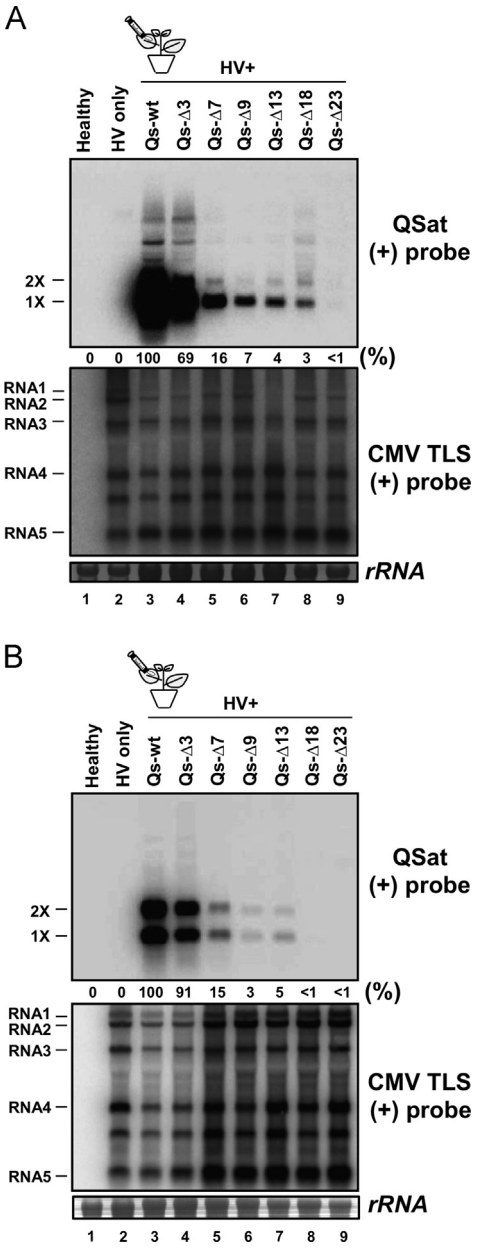

Fig. 3. Replication of Qsat variants in agroinfiltrated plants. Northern blot analysis of replication competence of Qsat deletion mutants in the presence of helper virus (HV) in (A) local and (B) systemically infected leaves of *N. benthamiana* plants. Following agroinfiltration with a mixture of indicated agrotransformants, duplicated blots containing total RNA isolated at 4 dpi (local) and 15 dpi (systemic) were subjected to hybridization as described under Fig. 2 legend. The positions of Qsat RNA monomeric (1 ×) and dimeric (2 ×) and RNA1 to RNA5 of helper virus are indicated on the left of each panel. Riboprobes used for hybridization are shown on the right of each panel. rRNA represent a loading control. Accumulation levels (%) of Qsat RNA below the upper panel were normalized against wt Qsat (100%).

(8 of 10 clones) of the Qs-Δ7 progeny recovered from systemically infected leaves contained $^{7}CGGACCC^{1}$, differing from wt by having a cytosine at position 7 (Table 1). This pattern of sequence heterogeneity resulting from 3′ end repair of the deleted sequences was evident in the progeny of the other two mutants (Qs-Δ9 and Qs-Δ13) as well (Table 1). The most sequence variation during 3′ end repair was observed for mutant Qs-Δ18 (Table 1). Of 18 nt deleted, the nt added during the repair process ranged between 5 to 13 nt. It is interesting to note that despite a low level of replication for mutants Qs-Δ9, Qs-Δ13 and Qs-Δ18 in infiltrated leaves (7%, 4% and 3% respectively; Fig. 3A), only the progeny of Qs-Δ9 and

Table 1
3′ end sequences of Qsat-RNA progeny generated in local and systemic leaves from wt and 3' end deletion mutants in the presence of helper virus.

Agro-clone	Local leaves[a]			Systemic leaves[b]		
	3' end sequence[c]	No. of bases added or deleted[d]	No. of clones[e]	3' end sequence[c]	No. of bases added or deleted[d]	No. of clones[e]
Qs-wt	[AUGUUUAUCAUUCCCUACCAGGACCC]			[AUGUUUAUCAUUCCCUACCAGGACCC]		
	AUGUUUAUCAUUCCCUACCAGGACCC	0	5/5	AUGUUUAUCAUUCCCUACCAGGACCC	0	
Qs-Δ3	[AUGUUUAUCAUUCCCUACCAGGA]	[−3]		[AUGUUUAUCAUUCCCUACCAGGA]	[−3]	
	AUGUUUAUCAUUCCCUACCAGGACCC	+3	10/10	AUGUUUAUCAUUCCCUACCAGGACCC*	+3	10/10
Qs-Δ7	[AUGUUUAUCAUUCCCUACC]	[−7]		[AUGUUUAUCAUUCCCUACC]	[−7]	
	AUGUUUAUCAUUCCCUACCGGGUCCC	+7	5/10	AUGUUUAUCAUUCCCUACCCGGACCC*	+7	8/10
	AUGUUUAUCAUUCCCUACCGGGUCC	+6	3/10	AUGUUUAUCAUUCCCUACCCGGACC	+6	2/10
	AUGUUUAUCAUUCCCUACCCGGACC	+6	1/10			
	AUGUUUAUCAUUCCCUACCCG	+2	1/10			
Qs-Δ9	[AUGUUUAUCAUUCCCUA]	[−9]		[AUGUUUAUCAUUCCCUA]	[−9]	
	AUGUUUAUCAUUCCCUAGGGACCC	+7	5/10	AUGUUUAUCAUUCCCUAAAGGACCC*	+8	4/10
	AUGUUUAUCAUUCCCCUUGGGACCC	+8	1/10	AUGUUUAUCAUUCCCUAGCUGGACCC	+9	3/10
	AUGUUUAUCAUUCCCUUCAGGCCC	+7	1/10	AUGUUUAUCAUUCCCUAUAGGACCC	+8	2/10
	AUGUUUAUCAUUCCCAACGGACCC	+7	1/10	AUGUUUAUCAUUCCCUACGGGACCC	+8	1/10
	AUGUUUAUCAUUACCC	−10	1/10			
Qs-Δ13	[AUGUUUAUCAUUC]	[−13]		[AUGUUUAUCAUUC]	[−13]	
	AUGUUUAUCAUUUCCC	+3	5/13	AUGUUUAUCAUUCGCUUGCCGACCC*	+12	8/15
	AUGUUUAUCAUUACCC	+3	3/13	AUGUUUAUCAUUCGCUUGCCC	+8	2/15
	AUGUUUAUCAUUGACCC	+4	1/13	AUGUUUAUCAUUCGCUUGCC	+7	1/15
	AUGUUUAUCAUUCGCUUGCCGACCC	+12	1/13	AUGUUUAUCAUUCGCUUGCCGAC	+10	1/15
	AUGUUUAUCAUUCUCACCCCAGAGACCC	+15	1/13	AUGUUUAUCAUUCGCUUGCCGACC	+11	1/15
	AUGUUUAUCAUUCUUCUAAGGAGACCC	+14	1/13	AUGUUUAUCAUUCGCUUGC	+6	1/15
	AUGUUUAUCAUUCUUCCUCGGACCC	+12	1/13	AUGUUUAUCAUUCCCCCGCCAGGACCC	+13	1/15
Qs-Δ18	[AUGUUUAU]	[−18]		[AUGUUUAU]	[−18]	
	AUGUUUAUUGGUACU	+7	4/16	None detected		
	AUGUUUAUUGGUACUGC	+9	4/16			
	AUGUUUAUUGGUACCC	+8	3/16			
	AUGUUUAUAUUGCUCCC	+9	2/16			
	AUGUUUAUUGGUACUGCUUUC	+13	1/16			
	AUGUUUAUUGGUACUUC	+9	1/16			
	AUGUUUAUUUCCC	+5	1/16			
Qs-Δ23	[AUG]	[−23]		[AUG]	[−23]	
	None detected			None detected		

[a] Plants were infiltrated with each indicated Q-sat agrotransformant in the presence of helper virus.
[b] Two weeks post infiltration, un-infiltrated systemically infected upper leaves were processed to recover Q-sat progeny as described under Materials and methods section.
[c] Qsat progeny RNA recovered from either local (at 4 dpi) or systemic leaves (at 15 dpi) were subjected RT-PCR followed by cloning and sequencing as described under Materials and methods section. 3′ end sequences harboring the engineered terminal deletions in each agroconstruct used to infiltrate are shown in brackets.
[d] Number of added or deleted bases in Q-sat progeny during in vivo repair process is shown respectively as (+) and (−). Number of terminal bases deleted in each mutant is shown in bracket.
[e] Total number of clones sequenced (denominator) and the number of clones with repaired sequence (numerator) is shown.

Qs-Δ13 was competent to move systemically (Fig. 3B). Although satRNAs have been shown to spread in non-encapsidated form (Moriones et al., 1992), the reason why the progeny of Qs-Δ18 failed to move systemically is currently unknown. Mutant Qs-Δ23 remained inactive throughout this study and no evidence for repair of the deleted nts was obtained (Table 1).

Effect of structural mutations introduced into the 3′ end of Q-satRNA on sequence repair

The observation that the repaired 3′-end sequences were heterogeneous led us to find answers to the following two questions: (i) does sequence restoration occur randomly? (ii) What factors would influence the sequence heterogeneity found in the repaired 3′-ends? Since the 3′ end of Q-satRNA was predicted to exhibit a high secondary structure (Gordon and Symons, 1983), we first sought to compare the 3′ end secondary structural features of the progenies of the 3′ terminal deletion mutants with that of Qs-wt (Fig. 4A) and mutant inocula (Fig. 4B). To this end, we employed an RNA folding program as described in Materials and methods section to predict the 3′ end secondary structures of the representative progenies that were detected most frequently in the systemically infected leaves (marked as asterisks on Table 1). Interestingly, despite sequence variation (Table 1), the in silico 3′ end secondary structures of the analyzed progenies were predicted to fold into similar structures to that of wt (a stem-loop structure with a big bulge). All mutant progeny displayed a characteristic folding maintaining an upper loop (UL) and an internal loop (IL) (Fig. 4C).

Next, we sought to examine whether the repair of the deletion mutations would not occur if the structural integrity of the Q-satRNA 3′ end were not disrupted by the engineered mutations. To verify this, we assembled a series of agroconstructs of Q-satRNA variants harboring deletions internally within the 3′ 19 nt region (Fig. 5A). Each of these internal deletions was designed specifically to either maintain or disrupt the in vitro 3′ end secondary structure of wt Q-satRNA (Fig. 4A). Among the six internal deletion mutants assembled, three mutants, Qs-Δ8–9, Qs-Δ10–12 and Qs-Δ16–18, were designed to maintain the secondary structure identical to that of wt (having the UL and IL; Fig. 5B) while the remaining three mutants, Qs-Δ4–7, Qs-Δ13–15 and Qs-Δ10–18, were designed to disrupt or destroy the internal loop structure (Fig. 5B). Each mutant was co-expressed with helper virus in *N. benthamiana* leaves via agroinfiltration. At 4 dpi, total RNAs were extracted from the local leaves and subjected to Northern blot analysis. It is interesting to note that three of the six mutants,

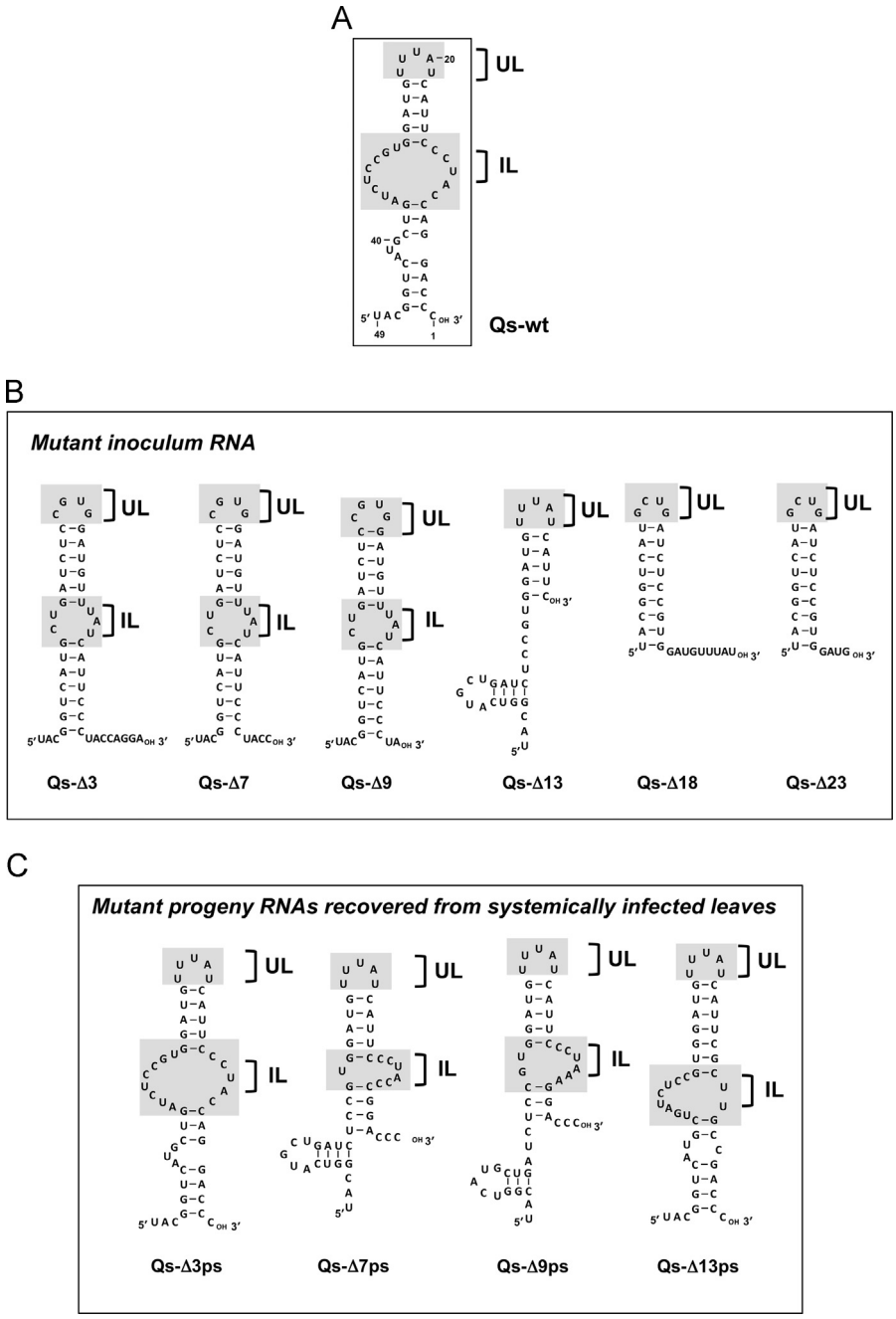

Fig. 4. Predicted secondary structures of Qsat RNA. Schematic representation of predicted in silico secondary structure of 3′ 49 nt region in (A) Qsat wt, (B) indicated 3′ deletion mutants inocula and (C) progeny of indicated mutants recovered from systemically infected leaves. In panel C, shaded regions indicate restoration of upper loop (UL) and internal loop (IL) at identical location.

Qs-Δ8–9, Qs-Δ10–12 and Qs-Δ16–18 (Fig. 5B) that maintained the wt secondary structure (specifically the UL and IL shown in Fig. 5B) were able to replicate and accumulate to detectable levels although they never reached wt levels (31–48% of wt; Fig. 6A). These results suggest the high level of structural flexibility tolerated by the satRNA. The other three mutants that failed to maintain the secondary structure (i.e. Qs-Δ4–7, Qs-13–15 and Qs-Δ10–18; Fig. 5B), did not replicate efficiently and accumulated $<5\%$ of wt (Fig. 6A).

To verify whether these internal deletions are preserved or repaired during subsequent replication leading to systemic spread, two weeks after agroinfiltration, we analyzed the systemically infected leaves with respect to accumulation levels of each mutant by Northern blot hybridization. Results are shown in Fig. 6B. The most striking observation is the significant increase in the replication of mutant Qs-Δ4–7. In contrast to a low level of replication ($<4\%$) in the local leaves (Fig. 6A), mutant Qs-Δ4–7 replicated efficiently and accumulated to 67% (compare lanes 2 in Fig. 6A and B) in systemically infected leaves. No significant change in accumulation was observed for other mutants that replicated $<1\%$ (i.e. Qs-Δ13–15 and Qs-Δ10–18; lanes 5 and 7 respectively in Fig. 6B).

The unexpected altered replication profile observed for mutant Qs-Δ4–7 in systemically infected leaves suggested that deletion of 4–7 nt could have been restored. To verify this possibility, we sequenced the progenies of all six mutants accumulated in local

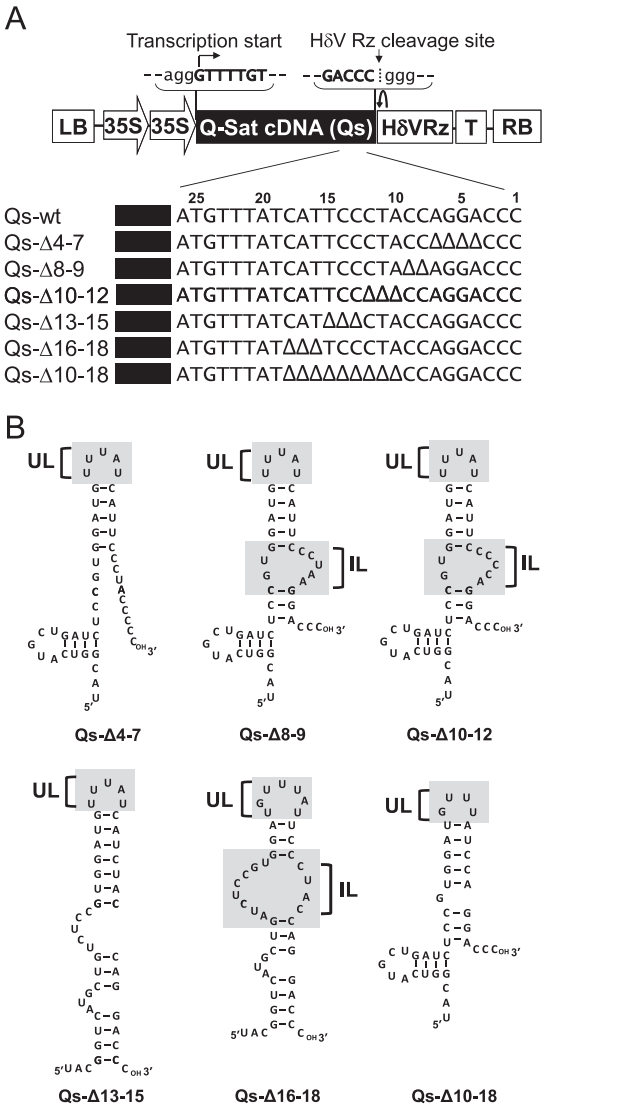

Fig. 5. Engineering the 3′-most internal deletions in Qsat RNA. (A) Schematic representation of internal deletions engineered into the Qsat agrotransformant. The genetic make up of the agrotransformant is described under Fig. 1 legend. Wild type sequence of the 3′ 26 nt region in Qsat (Qs-wt) is shown. In each Qsat variant, deleted. nucleotides are indicated by Δ. For example, in Qs-Δ4–7, ^{4}AGGA^{7} are deleted. (B) Predicted in silico secondary structures of Qsat variants shown in A. Shaded regions indicate preservation of stem-loop structures with internal bulge region. The location of upper loop (UL) and internal loop (IL) structures are indicated.

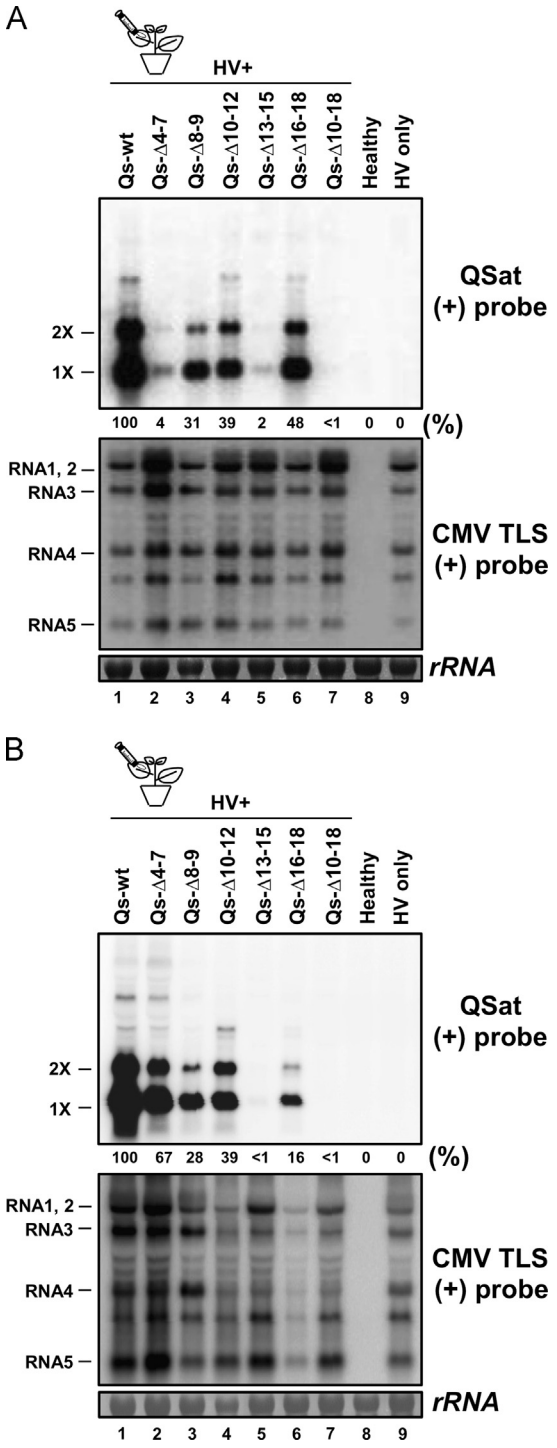

Fig. 6. Replication of Qsat internal deletion mutants. Northern blot analysis of replication competence of Qsat internal deletion mutants in the presence of helper virus in (A) local and (B) systemically infected leaves of *N. benthamiana* plants. Following agroinfiltration with a mixture of indicated agrotransformants, duplicated blots containing total RNA isolated at 4 dpi (local) and 15 dpi (systemic) were subjected to hybridization as described under Fig. 2 legend. The positions of Qsat RNA monomeric (1 ×) and dimeric (2 ×) and RNA1 to RNA5 of helper virus are indicated on the left of each panel. Riboprobes used for hybridization are shown on the right of each panel. rRNA represent a loading control. Accumulation levels (%) of each Qsat variant progeny RNA were normalized against wt Qsat (100%) and are shown at the bottom of each upper panel.

and systemically infected leaves. The results are summarized in Table 2. In local leaves, for mutant Qs-Δ4–7, nearly 75% of the progeny (9 of 12 clones) contained 3′ truncations ranging between 6 to 11 nt. The remaining 25% (3 of 12 clones) albeit heterogeneous, exhibited restoration of intact 3′ terminal sequence having one extra nt than wt. (see Table 2 for details). Although restoration of the deleted four nt was apparent in the progeny recovered from systemically infected leaves, 80% (8 of 10 clones) contained one extra nt than wt while the remaining 20% (2 of 10 clones) were identical to that of wt (Table 1). Among the remaining five mutants (i.e. Qs-Δ8–9, Qs-10–12, Qs-Δ13–15, Qs-Δ16–18 and Qs-Δ10–18), of specific interest are those mutants that maintained the secondary structure i.e. Qs-Δ8–9, Qs-Δ10–12, and Qs-Δ16–18. Despite maintenance of the secondary structure and competence to replicate, in each of these mutants the engineered deletions were preserved during replication in infiltrated and systemically infected leaves (Table 2). No restoration of engineered deletions was observed for mutants that failed to maintain the secondary structure i.e. Qs-Δ13–15 and Qs-Δ10–18. The significance of these observations is considered under the Discussion section.

Table 2
3′ end sequences of Qsat-RNA progeny generated in local and systemic leaves from 3' end internal deletion mutants in the presence of helper virus.

Agro-clone	Local leaves[a]			Systemic leaves[b]		
	3′end sequence[c]	No. of bases added or deleted[d]	No. of clones[e]	3′end sequence[c]	No. of bases added or deleted[d]	No. of clones[e]
Qs-wt	[AUGUUUAUCAUUCCCUACCAGGACCC]			[AUGUUUAUCAUUCCCUACCAGGACCC]		
Qs-Δ4-7	[AUGUUUAUCAUUCCCUACCΔΔΔΔCCC]	[−4]		[AUGUUUAUCAUUCCCUACCΔΔΔΔCCC]	[−4]	
	AUGUUUAUCAUUCCCUA	−9	3/12	AUGUUUAUCAUUCCCUACCGAGGACCC	+1	6/10
	AUGUUUAUCAUUCCCUACC	−7	2/12	AUGUUUAUCAUUCCCUACCCAGGACCC	+1	2/10
	AUGUUUAUCAUUCCCUACCC	−6	2/12	AUGUUUAUCAUUCCCUACCAGGACCC	0	2/10
	AUGUUUAUCAUUCCCUACCUCGGACCC	+1	2/12			
	AUGUUUAUCAUUCCC	−11	1/12			
	AUGUUUAUCAUUCCCUACCCGGCCC	-6	1/12			
	AUGUUUAUCAUUCCCUACCCGAGGACC	+1	1/12			
Qs-Δ8-9	[AUGUUUAUCAUUCCCUAΔΔAGGACCC]	[−2]		[AUGUUUAUCAUUCCCUAΔΔAGGACCC]	[−2]	
	AUGUUUAUCAUUCCCUAAGGACCC	−2	10/10	AUGUUUAUCAUUCCCUAAGGACCC	−2	10/10
Qs-Δ10-12	[AUGUUUAUCAUUCCΔΔΔCCAGGACCC]	[−3]		[AUGUUUAUCAUUCCΔΔΔCCAGGACCC]	[−3]	
	AUGUUUAUCAUUCCCCAGGACCC	−3	10/10	AUGUUUAUCAUUCCΔΔΔCCAGGACCC	−3	10/10
Qs-Δ13-15	[AUGUUUAUCAUΔΔΔCUACCAGGACCC]	[−3]		[AUGUUUAUCAUΔΔΔCUACCAGGACCC]	[−3]	
	AUGUUUAUCAUCUACCAGGACCC	−3	5/10	None detected		
	AUGUUUAUCAUCUACCAGGACC	−4	3/10			
	AUGUUUAUCAUCU	−13	2/10			
Qs-Δ16-18	[AUGUUUAUΔΔΔUCCCUACCAGGACCC]	[−3]		[AUGUUUAUΔΔΔUCCCUACCAGGACCC]	[−3]	
	AUGUUUAUUCCCUACCAGGACCC	−3	10/10	AUGUUUAUUCCCUACCAGGACCC	−3	10/10
Qs-Δ10-18	[AUGUUUAUΔΔΔΔΔΔΔΔΔCCAGGACCC]	[−9]		[AUGUUUAUΔΔΔΔΔΔΔΔΔCCAGGACCC]	[−9]	
	None detected			None detected		

[a] Plants were infiltrated with each indicated agrotransformant Q-sat in the presence of helper virus.
[b] Two weeks post infiltration, un-infiltrated systemically infected upper leaves were processed to recover Q-sat progeny as described under Materials and methods section.
[c] Qsat progeny RNA recovered from either local (at 4 dpi) or systemic leaves (at 15 dpi) were subjected RT-PCR followed by cloning and sequencing as described under Materials and methods section. 3′ end sequences harboring the engineered internal deletions in each agroconstruct used to infiltrate are shown in brackets.
[d] Number of added or deleted bases in Q-sat progeny during in vivo repair process is shown respectively as (+) and (−). Number of internal bases deleted in each mutant is shown in bracket.
[e] Total number of clones sequenced (denominator) and the number of clones with repaired sequence (numerator) is shown.

Discussion

The major focus of this study is to understand the 3′ end repair in Q-satRNA mediated by its helper virus replicase. Our results are in agreement with a previous study (Burgyan and Garcia-Arenal, 1998) that Q-3′end repair in Q-satRNA is mediated exclusively by helper virus replicase. However, in contrast to the previous study (Burgyan and Garcia-Arenal, 1998) that showed deletions up to 7 nt from the 3′ proximal regions of satRNA are repaired during helper virus-dependent replication in planta, we found that deletions up to 18 nt are repaired. Most importantly, our study shows that deletions internal to the 3′ proximal region could also be repaired and such repair mechanism selects for progeny having an optimal 3′ structural integrity. The significance of these observations in relation to 3′ end repair in viral RNA is discussed below.

Agroinfiltration vs mechanical inoculation

Our study revealed that the extent of the 3′ end repair of Q-satRNA by its helper virus replicase is influenced by the method used to deliver the inoculum. For example, as discussed under introduction, agroinfiltration offers synchronized delivery and co-expression of multiple plasmids to the same cell and transgene expression was observed in up to 90% of the cells encompassing the infiltrated leaf surface (Annamalai and Rao, 2005; Kapila et al., 1997). This trait is particularly attractive for studying multiple component viruses such as CMV and its satRNA. Furthermore, the fact that plasmids delivered via agroinfiltration are competent to generate mRNAs for up to 7 days (Kapila et al., 1997) results in a sustained availability of mutant transcripts for repair by viral replicase. By contrast, mechanical inoculation with optimal inoculum concentration limits the number of cells receiving the required constellation of viral components to initiate replication. Furthermore, the relative stability of 3′ deletion mutants of Q-satRNA varied depending on the length of the engineered deletion (Fig. 2A). This necessitates co-localization of Q-satRNA and helper virus to the same cell to initiate immediate 3′ repair. Consequently, in mechanically inoculated leaves, cells that receive only Q-satRNA deletion mutants are rapidly degraded by nucleases beyond repair even if helper virus is transported to the same cell at a later time point. This perhaps explains why Q-satRNA deletion mutants extending beyond the 3′-most-7 nucleotides are repaired by helper virus replicase in agroinfiltrated (Fig. 3) but not in mechanically inoculated plants (Fig. 2D) (Burgyan and Garcia-Arenal, 1998) (see below).

Significance of Q-satRNA structural integrity to replication

Our results accentuate the significance of the structural integrity required for the replication of Q-satRNA. For example, it is apparent from our sequence analysis and compilation of in silico secondary structures of Q-sat progeny corresponding to either 3′ terminal mutants (Fig. 3C Qs-Δ3 ps, Qs-Δ7 ps, Qs-Δ9p and, Qs-Δ13 ps) or internal deletion mutants (Fig. 4B; Qs-Δ8–9; Qs-Δ10–12 and Qs-Δ16–18) that only the progeny that retained intact secondary structure resulting from addition of heterologous nucleotides replicated and accumulated to detectable levels in local (Figs. 3 and 6A) and systemically infected leaves (Figs. 3 and 6B). Mutants that failed to maintain the required secondary structure (e.g. Fig. 5B, Qs-Δ13–15 and Qs-Δ10–18) failed to support the helper virus-dependent replication (Fig. 6A). To further shed light on the biological relevance of the 3′secondary structure feature seen in Q-sat, the in vitro 3′ secondary structures of five additional satRNAs (B2, B3, G, WL1, Ix5 and D4) (Bernal and Garcia-Arenal, 1997; Garcia-Arenal et al., 1987; Moriones et al., 1992; Rodriguez-Alvarado and Roossinck, 1997) associated with other CMV strains, have been compared. These six satRNAs varied in their pathogenicity and differentially interacted with CMV and

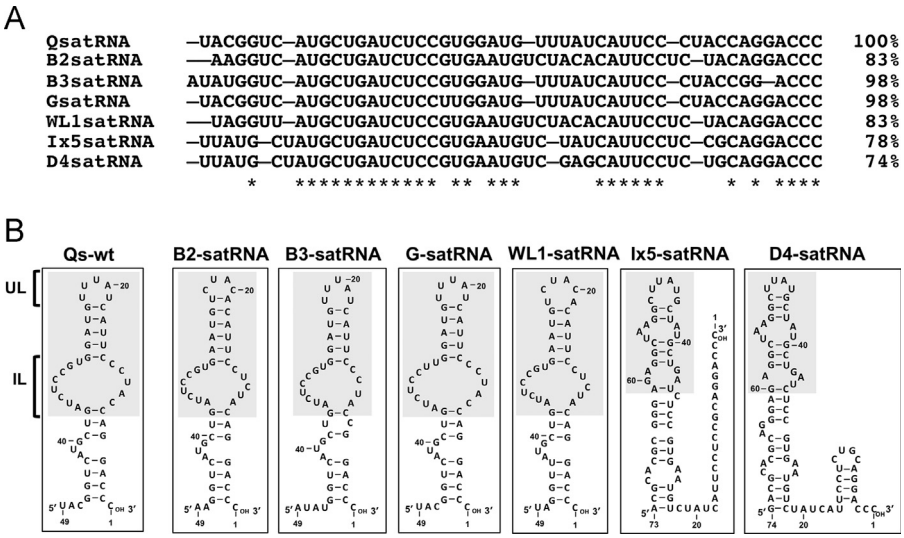

Fig. 7. Primary sequences and in vitro secondary structures of satRNAs associated with different CMV strains. (A) Primary sequences of the 3′ 49 nt regions of Q-sat and six other satRNA strains are shown. Percentage (%) of sequence similarity of other strains with respect to Q-sat (100%) is indicated. Asterisks indicate the conserved nucleotides among seven satRNAs. (B) In vitro secondary structures of satRNAs associated with different CMV strains (Bernal and Garcia-Arenal, 1997; Garcia-Arenal et al., 1987; Rodriguez-Alvarado and Roossinck, 1997). Shaded regions indicate highly conserved upper loop (UL) and internal loop (IL) structures.

TAV (Moriones et al., 1992). The primary sequence encompassing the 3′ 49 nt region of Q-sat shows extensive similarity to those of B3 and G-sat (98%), close similarity to those of B2 and WL1 (83%), and moderate similarity to those of Ix5 (78%) and D4-satRNA (74%) (Fig. 7A). A comparison of 3′ secondary structures of four satRNAs (i.e. B2, B3, G, WL1-satRNA) are identical to that of Q-sat, while that of Ix5 and D4-sat RNA are quite different (Fig. 7B). Nevertheless, all these seven satRNAs display highly conserved UP and IL structures (Fig. 7B). Collectively the data suggest that maintenance of the 3′ secondary structure is vital for helper virus-dependent satRNA replication.

Mechanism regulating the 3′ end repair in Q-satRNA

Previous in vivo studies revealed that several mechanisms are involved in repairing the 3′ terminal sequences of a wide range of satRNAs associated with plant viruses. Some of the mechanisms include recombination and abortive synthesis and priming as in satRNA of TCV (Carpenter and Simon, 1996a, b), telomerase-like activity as in the satRNA of Cymbidium rinspot virus (Dalmay et al., 1993) and template independent repair as in a satRNA of CMV (Burgyan and Garcia-Arenal, 1998). In this study, the rapidity of repair and efficient synthesis of progeny for Qs-Δ3, Qs-Δ7, Qs-Δ9 Qs-Δ13 and Qs-Δ18 demonstrates that active 3′ end turnover exists in plant cells. Results from a series of experiments shown in Fig. 2 clearly demonstrated that addition of nucleotides to generate biologically active mutant sequences is mediated by helper virus replicase but not due to the action of cellular polymerase.

Data from inoculations containing 3′ terminal deletions other than Qs-Δ3 (e.g. Qs-D7, Qs-Δ9, Qs-Δ13, Qs-Δ18 and Qs-Δ23; Fig. 1) or internal deletions (Qs-Δ8–9, Qs-Δ10–12, Qs-Δ13–15; Fig. 6A) provided insight to the mechanisms by which a most favorable sequence is restored to maintain the structural integrity. Absence of any sequences resembling that of helper virus genomic 3′ ends suggested that recombination was not involved (Tables 1 and 2). However, given the common secondary structure in the 3′ terminal structures between HV RNA3 and Q-satRNA (Gordon and Symons, 1983), we do not rule out a possible recombination between these two RNA species followed by a rapid selection of mutants that more closely resemble the Q-satRNA 3′ terminal sequences. Another likely source of sequence for regeneration of the functional Q-satRNA 3′ terminus is at or 3′ of the ribozyme. For example, if ribozyme cleavage occurred after exit from the nucleus, then the RNA sequences at the 3′ terminus could be used as possible source of RNA upon which the HV replicase initiated copying, albeit at low efficiency before selection of mutations occurred, closely resembling the Q-satRNA sequence. However, we rule out this possibility since sequencing data of the transiently expressed Q-satRNA mutants expressed in the absence of HV failed to reveal the presence of any non-viral sequences.

As discussed above, mechanical co-inoculation of transiently expressed mutant sequences and helper virus negated that misincorporation of nucleotides did not occur by cellular polymerase during transcription of T-DNA inserts. However, the lack of proof reading ability of viral RdRp leads to fluidity in RNA genomes and results in accumulation of quasispecies in viral progeny (Domingo et al., 1985). Thus, generation of replication-competent Q-satRNA progeny repair involving the addition of heterologous nucleotides could be attributed to polymerase error mediated by the helper virus replicase. This followed by the strong selection pressure effectively opts for a consensus sequence that could outcompete less favorable sequences. Since, minor nucleotide changes could significantly alter the pathogenicity and host specificity of satRNA (Sleat and Palukaitis, 1992), it will be of interest to verify whether Q-sat mutant progeny harboring heterologous nucleotides would persist or would be reverted to wild type or new pathogens during subsequent multiple passages.

Biological relevance of 3′ end repair

Replication of Q-sat is cytoplasmic since the replication of its helper virus is confined to the same cellular compartment. However, using cell biology based approaches we recently demonstrated Q-sat has a propensity to localize in the nucleus for a template independent addition of a hepta nucleotide motif at the monomer junctions to form multimers that subsequently serve as efficient templates for helper virus-dependent replication (Chaturvedi et al., 2013; Choi et al., 2012; Seo et al., 2013).

Since none of the six 3′ end deletion mutants are repaired by the cellular polymerase Fig. 2A–C), we hypothesize that 3′ end

repair, specifically addition of $-CCC_{OH}$, can only be mediated by the helper virus-encoded replicase and whereas nuclear encoded polymerases would add hepta nucleotide motif only to those Q-sat transcripts that terminated with-CCC_{OH}. Consequently, following transient expression in the nucleus, all 3′ terminal Q-sat mutant transcripts exit the cytoplasm to get repaired by the helper virus-replicase, generating RNA transcripts terminating in $-CCC_{OH}$ and re-enter the nucleus for the addition of hepta nucleotide motif and multimer formation as described above. Therefore it would be significant not only to identify the host factors involved in nuclear import of Q-sat (Chaturvedi et al., 2013) but also the Q-sat sequences that play an important role in this active process. Studies are in progress in our laboratory to resolve these issues.

Materials and methods

Virus, satRNA strain and construction of 3′ terminal mutant clones for agroinfiltration

Throughout this study, we used Q-CMV and its satRNA (Q-sat) (Gordon and Symons, 1983). The full-length cDNA clones for Q-Sat RNA 3′ terminal deletion mutants were amplified by PCR using a 5′ forward primer (5′-GTTTTGTTTGTTAGAGAATTG-3′) and each different 3′ reverse primer for each mutant as follows: 5′-TCCTGGTAGGGAATGATAA-3′ for Qs-Δ3; 5′-GGTAGGGAATGATAAACATC-3′ for Qs-Δ7; 5′-TAGGGAATGATAAACATCCAC-3′ for Qs-Δ9; 5′-GAATGATAAACATCCACGG-3′ for Qs-Δ13; 5′-ATAAACATCCACGGAGATCAG-3′ for Qs-Δ18; and 5′-CATCCACGGAGATCAGCATGAC-3′ for Qs-Δ23. To obtain the 3′ terminal internal deletion mutants, Qsat RNA were amplified by PCR using the same 5′ forward primer and the following 3′ reverse primers: 5′-GGGGGTAGGGAATGATAAACATC-3′ for Qs-Δ4–7; 5′-GGGTCCTTAGGGAATGATAAACATCCAC-3′ for Qs-Δ8–9; 5′-GGGTCCTGGGGAATGATAAACATCCACG-3′ for Qs-Δ10–12; 5′ GGGTCCTGGTAGATGATAAACATCCACGGAG-3′ for Qs-Δ13–15; 5′-GGGTCCTGGTAGGGAATAAACATCCACGGAGATCAGC-3′ for Qs-Δ16–18; and 5′-GGGTCCTGGATAAACATCCACGGAGATCAG-3′ for Qs-Δ10–18. PCR was carried out with $Vent_R^{®}$ DNA polymerase (New England Biolabs) to create a blunt end and its product was ligated into a binary vector (pCassHDV) digested with *Stu*I and *Nco*I, and treated with mung bean nuclease (New England Biolabs) to create blunt ends. The resulting clones were verified by sequencing. The agro-constructs and characteristic features for the three genomic RNAs of Q-CMV are as described previously (de Wispelaere and Rao, 2009).

Plant inoculations and RNA gel blots

For agroinfiltration, following transformation of binary vectors into *Agrobacterium tumefaciens* strain GV3101, agrotransformants were infiltrated into *N. benthamiana* plants as previously described (Annamalai and Rao, 2005). For mechanical inoculations, inocula were prepared by mixing approximately 50 μg/ml total RNA obtained from leaves agroinfiltrated with each mutant with 200 μg/ml of helper virus virion RNA. The total RNAs from either agroinfiltrated or mechanically inoculated plants were extracted using Trizol reagent (Invitrogen). Plus-strand progeny of wt and mutant Q-sat and QCMV was analyzed by Northern blot hybridization with ^{32}P-labeled strand specific riboprobes and quantitated as described previously (Seo et al., 2013). In each assay, 4–6 plants were inoculated and each experiment was repeated at least three times.

Analysis of 3′-terminal sequence of QsatRNA mutants

Five micrograms of total RNA, extracted from either mechanically inoculated or agroinfiltrated leaves at 4 dpi and systemically infected leaves at 15 dpi or virion RNA, were subjected to electrophoresis on 5% acrylamide-8 M urea gels. After being stained with ethidium bromide, the gel corresponding to the size of QsatRNA was excised and the RNA was eluted in buffer containing 0.5 M ammonium acetate, 1 mM EDTA, 0.1% SDS and then purified and precipitated (Kwon et al., 2005). The RNA was subjected to polyadenylation with *Escherichia coli* poly(A) polymerase (New England Biolabs). The poly(A)-tailed RNA was used as the template for reverse transcription with the following primer [5′-GGGAGGACACAGCCAACATACGTA$(T)_{17}$-3′]. The resulting cDNA was amplified by PCR using Crimson Taq DNA polymerase (New England Biolabs), a QsatRNA-specific primer (5′ forward primer as described above) and a reverse primer identical to that used for cDNA synthesis without the terminal poly(T). The resultant PCR products were cloned into pGEM-T Easy cloning vector (Promega) and sequenced.

Prediction of secondary structures of the 3′ terminal region for Qsat RNA mutants and progeny RNAs

The representative progenies that were detected most frequently in systemically infected leaves for 3′terminal deletion mutants and for 3′ terminal internal deletion mutants were analyzed for predicted RNA secondary structures using the mfold web server (http://mfold.rna.albany.edu/?q=mfold/RNA-Folding-Form)

Acknowledgments

We thank Shou-wei-Ding for providing cDNA clones of Q-CMV and Q-satRNA, Deb Mathews for editorial comments. This study was supported by a grant from Committee on Research of the Riverside Division of Academic Senate.

References

Annamalai, P., Rao, A.L., 2005. Replication-independent expression of genome components and capsid protein of brome mosaic virus in planta: a functional role for viral replicase in RNA packaging. Virology 338, 96–111.
Annamalai, P., Rofail, F., Demason, D.A., Rao, A.L., 2008. Replication-coupled packaging mechanism in positive-strand RNA viruses: synchronized coexpression of functional multigenome RNA components of an animal and a plant virus in *Nicotiana benthamiana* cells by agroinfiltration. J. Virol. 82, 1484–1495.
Bamunusinghe, D., Chaturvedi, S., Seo, J.K., Rao, A.L., 2013. Mutations in the capsid protein of Brome mosaic virus affecting encapsidation eliminate vesicle induction in planta: implications for virus cell-to-cell spread. J. Virol. 87, 8982–8992.
Bamunusinghe, D., Seo, J.K., Rao, A.L., 2011. Subcellular localization and rearrangement of endoplasmic reticulum by Brome mosaic virus capsid protein. J. Virol. 85, 2953–2963.
Bernal, J.J., Garcia-Arenal, F., 1997. Analysis of the in vitro secondary structure of cucumber mosaic virus satellite RNA. RNA 3, 1052–1067.
Boccard, F., Baulcombe, D., 1993. Mutational analysis of cis-acting sequences and gene function in RNA3 of cucumber mosaic virus. Virology 193, 563–578.
Bol, J.F., 2005. Replication of alfamo- and ilarviruses: role of the coat protein. Annu. Rev. Phytopathol. 43, 39–62.
Burgyan, J., Garcia-Arenal, F., 1998. Template-independent repair of the 3′ end of cucumber mosaic virus satellite RNA controlled by RNAs 1 and 2 of helper virus. J. Virol. 72, 5061–5066.
Carpenter, C.D., Simon, A.E., 1996a. In vivo repair of 3′-end deletions in a TCV satellite RNA may involve two abortive synthesis and priming events. Virology 226, 153–160.
Carpenter, C.D., Simon, A.E., 1996b. In vivo restoration of biologically active 3′ ends of virus-associated RNAs by nonhomologous RNA recombination and replacement of a terminal motif. J. Virol. 70, 478–486.
Chaturvedi, S., Kalantidis, K., Rao, A.L., 2013. A bromodomain containing host protein mediates the nuclear import of a satellite RNA of cucumber mosaic virus. J. Virol. , http://dx.doi.org/10.1128/JVI.03082-13.
Choi, S.H., Seo, J.K., Kwon, S.J., Rao, A.L., 2012. Helper virus-independent transcription and multimerization of a satellite RNA associated with cucumber mosaic virus. J. Virol. 86, 4823–4832.

Dalmay, T., Russo, M., Burgyan, J., 1993. Repair in vivo of altered 3′ terminus of cymbidium ringspot tombusvirus RNA. Virology 192, 551–555.
de Wispelaere, M., Rao, A.L., 2009. Production of cucumber mosaic virus RNA5 and its role in recombination. Virology 384, 179–191.
Ding, S.W., Anderson, B.J., Haase, H.R., Symons, R.H., 1994. New overlapping gene encoded by the cucumber mosaic virus genome. Virology 198, 593–601.
Ding, S.W., Rathjen, J.P., Li, W.X., Swanson, R., Healy, H., Symons, R.H., 1995. Efficient infection from cDNA clones of cucumber mosaic cucumovirus RNAs in a new plasmid vector. J. Gen. Virol. 76, 459–464.
Domingo, E., Martinez-Salas, E., Sobrino, F., de la Torre, J.C., Portela, A., Ortin, J., Lopez-Galindez, C., Perez-Brena, P., Villanueva, N., Najera, R., et al., 1985. The quasispecies (extremely heterogeneous) nature of viral RNA genome populations: biological relevance—a review. Gene 40, 1–8.
Dreher, T.W., 2009. Role of tRNA-like structures in controlling plant virus replication. Virus Res. 139, 217–229.
Garcia-Arenal, F., Palukaitis, P., 1999. Structure and functional relationships of satellite RNAs of cucumber mosaic virus. Curr. Top. Microbiol. Immunol. 239, 37–63.
Garcia-Arenal, F., Zaitlin, M., Palukaitis, P., 1987. Nucleotide sequence analysis of six satellite RNAs of cucumber mosaic virus: primary sequence and secondary structure alterations do not correlate with differences in pathogenicity. Virology 158, 339–347.
Gopinath, K., Kao, C.C., 2007. Replication-independent long-distance trafficking by viral RNAs in *Nicotiana benthamiana*. Plant Cell 19, 1179–1191.
Gordon, K.H., Symons, R.H., 1983. Satellite RNA of cucumber mosaic virus forms a secondary structure with partial 3′-terminal homology to genomal RNAs. Nucleic Acids Res. 11, 947–960.
Hema, M., Gopinath, K., Kao, C., 2005. Repair of the tRNA-like CCA sequence in a multipartite positive-strand RNA virus. J. Virol. 79, 1417–1427.
Hu, C.-C., Hsu, Y.-H., Lin, N.-S., 2009. Satellite RNAs and satellite viruses of plants. Viruses 1, 1325–1350.
Kapila, J., Rycke, R., Van Montagu, M., Angenon, G., 1997. An agrobacterium-mediated transient gene expression system for intact leaves. Plant Sci. 122, 101–108.
Kwon, S.J., Park, M.R., Kim, K.W., Plante, C.A., Hemenway, C.L., Kim, K.H., 2005. cis-Acting sequences required for coat protein binding and in vitro assembly of Potato virus X. Virology 334, 83–97.
Kwon, S.J., Rao, A.L., 2012. Emergence of distinct brome mosaic virus recombinants is determined by the polarity of the inoculum RNA. J. Virol. 86, 5204–5220.
Li, H., Li, W.X., Ding, S.W., 2002. Induction and suppression of RNA silencing by an animal virus. Science 296, 1319–1321.
Marillonnet, S., Giritch, A., Gils, M., Kandzia, R., Klimyuk, V., Gleba, Y., 2004. In planta engineering of viral RNA replicons: efficient assembly by recombination of DNA modules delivered by Agrobacterium. Proc. Nat. Acad. Sci. U.S.A. 101, 6852–6857.
Mori, M., Mise, K., Kobayashi, K., Okuno, T., Furusawa, I., 1991. Infectivity of plasmids containing brome mosaic virus cDNA linked to the cauliflower mosaic virus 35S RNA promoter. J. Gen. Virol. 72, 243–246.
Moriones, E., Diaz, I., Rodriguez-Cerezo, E., Fraile, A., Garcia-Arenal, F., 1992. Differential interactions among strains of tomato aspermy virus and satellite RNAs of cucumber mosaic virus. Virology 186, 475–480.
Nagy, P.D., Carpenter, C.D., Simon, A.E., 1997. A novel 3′-end repair mechanism in an RNA virus. Proc. Nat. Acad. Sci. U.S.A. 94, 1113–1118.
Palukaitis, P., Garcia-Arenal, F., 2003. Cucumoviruses. Adv. Virus Res. 62, 241–323.
Racaniello, V.R., Baltimore, D., 1981. Cloned poliovirus complementary DNA is infectious in mammalian cells. Science 214, 916–919.
Rao, A.L., Dreher, T.W., Marsh, L.E., Hall, T.C., 1989. Telomeric function of the tRNA-like structure of brome mosaic virus RNA. Proc. Nat. Acad. Sci. USA 86, 5335–5339.
Rao, A.L., Hall, T.C., 1993. Recombination and polymerase error facilitate restoration of infectivity in brome mosaic virus. J. Virol. 67, 969–979.
Rodriguez-Alvarado, G., Roossinck, M.J., 1997. Structural analysis of a necrogenic strain of cucumber mosaic cucumovirus satellite RNA in planta. Virology 236, 155–166.
Seo, J.K., Kwon, S.J., Chaturvedi, S., Ho Choi, S., Rao, A.L., 2013. Functional significance of a hepta nucleotide motif present at the junction of cucumber mosaic virus satellite RNA multimers in helper-virus dependent replication. Virology 435, 214–219.
Shimura, H., Pantaleo, V., Ishihara, T., Myojo, N., Inaba, J., Sueda, K., Burgyan, J., Masuta, C., 2011. A viral satellite RNA induces yellow symptoms on tobacco by targeting a gene involved in chlorophyll biosynthesis using the RNA silencing machinery. PLoS Pathog. 7, e1002021.
Simon, A.E., Roossinck, M.J., Havelda, Z., 2004. Plant virus satellite and defective interfering RNAs: new paradigms for a new century. Annu. Rev. Phytopathol. 42, 415–437.
Sleat, D.E., Palukaitis, P., 1992. A single nucleotide change within a plant virus satellite RNA alters the host specificity of disease induction. Plant J.: Cell Mol. Biol. 2, 43–49.
Smith, N.A., Eamens, A.L., Wang, M.B., 2011. Viral small interfering RNAs target host genes to mediate disease symptoms in plants. PLoS Pathog. 7, e1002022.
Wang, M.B., Bian, X.Y., Wu, L.M., Liu, L.X., Smith, N.A., Isenegger, D., Wu, R.M., Masuta, C., Vance, V.B., Watson, J.M., Rezaian, A., Dennis, E.S., Waterhouse, P.M., 2004. On the role of RNA silencing in the pathogenicity and evolution of viroids and viral satellites. Proc. Nat. Acad. Sci. U.S.A. 101, 3275–3280.
Weber, H., Haeckel, P., Pfitzner, A.J., 1992. A cDNA clone of tomato mosaic virus is infectious in plants. J. Virol. 66, 3909–3912.
Weiner, A.M., Maizels, N., 1987. tRNA-like structures tag the 3′ ends of genomic RNA molecules for replication: implications for the origin of protein synthesis. Proc. Nat. Acad. Sci. U.S.A. 84, 7383–7387.
Yi, G., Letteney, E., Kim, C.H., Kao, C.C., 2009. Brome mosaic virus capsid protein regulates accumulation of viral replication proteins by binding to the replicase assembly RNA element. RNA 15, 615–626.